JOURNAL OF AGRICULTURAL AND FOOD CHEMISTRY

Article

pubs.acs.org/JAFC

Xanthohumol, a Polyphenol Chalcone Present in Hops, Activating Nrf2 Enzymes To Confer Protection against Oxidative Damage in PC12 Cells

Juan Yao, Baoxin Zhang, Chunpo Ge, Shoujiao Peng, and Jianguo Fang*

State Key Laboratory of Applied Organic Chemistry and College of Chemistry and Chemical Engineering, Lanzhou University, Lanzhou, Gansu 730000, China

Supporting Information

ABSTRACT: Xanthohumol (2′,4′,4-trihydroxy-6′-methoxy-3′-prenylchalcone, Xn), a polyphenol chalcone from hops (*Humulus lupulus*), has received increasing attention due to its multiple pharmacological activities. As an active component in beers, its presence has been suggested to be linked to the epidemiological observation of the beneficial effect of regular beer drinking. In this work, we synthesized Xn with a total yield of 5.0% in seven steps and studied its neuroprotective function against oxidative-stress-induced neuronal cell damage in the neuronlike rat pheochromocytoma cell line PC12. Xn displays moderate free-radical-scavenging capacity in vitro. More importantly, pretreatment of PC12 cells with Xn at submicromolar concentrations significantly upregulates a panel of phase II cytoprotective genes as well as the corresponding gene products, such as glutathione, heme oxygenase, NAD(P)H:quinone oxidoreductase, thioredoxin, and thioredoxin reductase. A mechanistic study indicates that the α,β-unsaturated ketone structure in Xn and activation of the transcription factor Nrf2 are key determinants for the cytoprotection of Xn. Targeting the Nrf2 by Xn discloses a previously unrecognized mechanism underlying the biological action of Xn. Our results demonstrate that Xn is a novel small-molecule activator of Nrf2 in neuronal cells and suggest that Xn might be a potential candidate for the prevention of neurodegenerative disorders.

KEYWORDS: *xanthohumol, oxidative stress, antioxidant, neuroprotection, Nrf2*

INTRODUCTION

In aerobes, a small part of oxygen is physiologically metabolized to reactive oxygen species (ROS), which generally serve as messenger molecules to regulate diverse signaling pathways involved in cell differentiation, proliferation, and death.[1,2] Oxidative stress, arising from uncontrolled production of ROS beyond the neutralizing capacity of the cellular antioxidant defense system, causes deleterious effects and oxidative damage to various cellular components, such as lipids, proteins, and nucleic acids.[1] As neuronal cells are particularly vulnerable to oxidative stress and have limited replenishment during the entire lifespan, increasing evidence has supported oxidative stress as one of the pathogenic causes in the neuropathology of adult neurodegenerative disorders such as Alzheimer's disease and Parkinson's disease.[1,3] Supplementation of antioxidants or stimulation of the cellular endogenous antioxidant defense system could efficiently block or retard the process of such diseases. The latter approach is preferred as such action is sustained and is regulated at the transcriptional level. A well-deciphered and universal pathway to induce cellular intrinsic antioxidant defense involves the transcription factor NF-E2-related factor 2 (Nrf2)-mediated upregulation of a set of cytoprotective genes ("phase II" genes).[4] Under basal conditions, the cytosolic regulatory protein Kelch-like ECH-associated protein 1 (Keap1) binds tightly to Nrf2, retaining it in the cytoplasm and directing it to proteasome degradation.[5] The association of Keap1 with Nrf2 critically relies on the cysteine residue(s) in the protein Keap1. Stimulants that could modify such cysteine residue(s) cause the dissociation of Nrf2 from the inhibitory partner Keap1 and facilitate Nrf2 to translocate into the nucleus, where Nrf2 binds to the antioxidant-responsive element (ARE) consensus sequence to initiate the transcription of phase II genes.[6] In this sense, activation of the Nrf2−ARE pathway is a promising therapeutic approach in neurodegenerative diseases. Thus, the past years have witnessed expanding endeavors in identifying and developing naturally occurring or synthetic small-molecule activators of the Nrf2−ARE pathway as potential neuroprotective agents.[7]

Hops (*Humulus lupulus* L.), from the dried female clusters of the hop plant, are widely used in beers and a few types of soft drinks, such as Julmust and Malta. In traditional Chinese medicine, hops have been used to treat a variety of ailments for centuries. Xanthohumol (2′,4′,4-trihydroxy-6′-methoxy-3′-prenylchalcone, Xn), a structurally simple polyphenol chalcone that occurs only in the hop plants, is the principal prenylated flavonoid in hops (up to 1% based on dry weight) and is present in micromolar concentrations in beers.[8,9] The presence of a high concentration of Xn in beers might be linked to the epidemiological observation of the beneficial effect of regular beer drinking.[10] Xn has attracted considerable interest because of its multiple pharmacological functions,[8,11] including antioxidation,[12] cadiovascular protection,[13] anticancer and

Received: October 20, 2014
Revised: January 7, 2015
Accepted: January 14, 2015

DOI: 10.1021/jf505075n
J. Agric. Food Chem. XXXX, XXX, XXX−XXX

cancer chemoprevention,[14−18] antivirus,[19] antiobesity,[20,21] and anti-inflammation.[15,22] Nevertheless, the investigation of this pleiotropic molecule on the neuronal system has only been limitedly cultivated,[23] and the underlying mechanism of the action has not been well elucidated.

As our continued efforts in discovering and developing novel redox-active small molecules as potential therapeutic agents,[24−30] we synthesized Xn and investigated its cytoprotection and the underlying mechanism in a neuronlike rat pheochromocytoma cell line, PC12. Xn was prepared from the readily available starting materials in seven steps with a total yield of 5.0%. As a polyphenolic compound, Xn moderately scavenges free radicals in vitro. Moreover, Xn efficiently activates the Nrf2−ARE signaling pathway at submicromolar concentrations in PC12 cells, leading to upregulation of a panel of phase II enzyme expression and remarkable protection of the cells from hydrogen peroxide (H_2O_2)- or 6-hydroxydopamine (6-OHDA)-induced neurotoxicity. We further clarified that the potential neuroprotection of Xn is dependent on both the α,β-unsaturated ketone moiety within Xn and the activation of transcription factor Nrf2. Our results demonstrate, for the first time, that Xn is a small-molecule activator of the Nrf2−ARE pathway in neuronal cells and suggest that Xn might be a potential candidate for the prevention of neurodegeneration. The structural determinant of such cytoprotection sheds light on designing and developing novel therapeutic agents.

■ MATERIALS AND METHODS

Materials. Dulbecco's modified Eagle's medium (DMEM), *N*-acetyl-Asp-Glu-Val-Asp-*p*-nitroanilide (Ac-DEVD-pNA), G418 disulfate salt, dimethyl sulfoxide (DMSO), yeast glutathione reductase (GR), Hoechst 33342, and 2′,7′-dichlorfluorescein diacetate (DCFH-DA) were obtained from Sigma-Aldrich (St. Louis, MO). NADPH was obtained from Roche (Mannheim, Germany). 2,2′-Azinobis(3-ethylbenzthiazoline-6-sulfonic acid) (ABTS), 2,6-dichlorophenol indophenol (DCPIP), 2,2′-azobis(2-methylpropionamidine) dihydrochloride (AAPH), *tert*-butylhydroquinone (tBHQ), and β-NADH were purchased from Sigma-Aldrich. Fetal bovine serum (FBS) was obtained from HyClone, Thermo Fisher Scientific (Waltham, MA). The recombinant rat TrxR1, which has a specific activity of 50% of that of the wild-type rat TrxR1 with the DTNB assay, was a gift from Prof. Arne Holmgren at Karolinska Institute, Sweden. *Escherichia coli* Trx was purchased from IMCO (Stockholm, Sweden, www.imcocorp.se). Anti-TrxR1 antibody was obtained from Santa Cruz Biotechnology (Santa Cruz, CA). 3-(4,5-Dimethylthiazol-2-yl)-2,5-diphenyltetrazolium bromide (MTT), penicillin, and streptomycin were obtained from Amresco (Solon, OH). Bovine serum albumin (BSA), phenylmethanesulfonyl fluoride (PMSF), sodium orthovanadate (Na_3VO_4), and antilamin and antiactin antibodies were obtained from Beyotime (Nantong, China). 5,5′-Dithiobis(2-nitrobenzoic acid) (DTNB) was obtained from J&K Scientific (Beijing, China). 6-Hydroxydopamine hydrobromide (6-OHDA), anti-TrxR1 antibody, anti-Trx1 antibody, and anti-Nrf2 antibody were from Santa Cruz Biotechnology. Anti-HO-1 antibody and anti-NQO1 antibody were obtained from Sangon Biotech (Shanghai, China). The shRNA plasmids targeting coding regions of the rat Nrf2 gene (shNrf2) and the control nontargeting shRNA (shNT) were purchased from GenePharma Co., Ltd. (Shanghai, China). GeneTran III transfection reagent was obtained from Biomiga (San Diego, CA). All other reagents were of analytical grade.

In Vitro Antioxidant Activity of Xn. *ABTS Free-Radical-Scavenging Activity.* The $ABTS^{\bullet+}$ scavenging capacity was determined according to the published method.[27] The $ABTS^{\bullet+}$ radical cation solution, which was prepared from oxidation of ABTS (7 mM) by potassium persulfate (2.5 mM) for 12−16 h in the dark at room temperature, was diluted to an absorbance of 0.700 ± 0.020 at 734 nm. The $ABTS^{\bullet+}$ solution (2 mL) and the antioxidant solution (100 μL) were mixed and incubated at room temperature. After 30 min, the absorbance at 734 nm was determined. The absorbance of the free radical solution without Xn was divided by that with 40 μM Xn to give the percentage of the remaining free radicals.

Assay of Thiobarbituric Acid Reactive Substances (TBARSs). The erythrocyte ghost, prepared following the published procedures,[27] was diluted to a final protein concentration of 0.96 mg/mL and incubated at 37 °C in 0.1 M PBS (pH 7.4). The lipid peroxidation was initiated by the addition of AAPH in the presence or absence of Xn (40 μM). The reaction mixture was gently shaken at 37 °C for 30 min. The reaction mixture was taken out, and a TCA−TBA−HCl stock solution (15% (w/v) trichloroacetic acid, 0.375% (w/v) TBA, 0.25 M HCl) was added, together with 0.02% (w/v) BHT. This amount of BHT completely prevents the formation of any nonspecific TBARS from the decomposition of AAPH during the subsequent boiling. The resulting mixture was heated in a boiling water bath for 15 min. After cooling, the precipitate was removed by centrifugation. TBARS in the supernatant was quantified at 532 nm using an extinction coefficient of $1.56 \times 10^5\ M^{-1}\ cm^{-1}$.[27]

Cell Cultures. The rat adrenal pheochromocytoma cell line PC12 was obtained from the Shanghai Institute of Biochemistry and Cell Biology, Chinese Academy of Sciences. The cells were cultured in DMEM medium supplemented with 10% FBS, 2 mM glutamine, and 100 units/mL penicillin/streptomycin and maintained in a humidified atmosphere with 5% CO_2 at 37 °C. The generation of Nrf2-knockdown PC12 cells is described in the following section.

Cytotoxicity Assays. *MTT Assay.* To investigate the cytotoxicity of Xn on PC12 cells, the cells were seeded at a density of 1×10^4 cells/well in 96-well plates for 24 h followed by incubation with Xn or other agents for 24 h at 37 °C in a final volume of 100 μL. For the H_2O_2 or 6-OHDA injury model, PC12 cells (1×10^4 cells/well) were plated in a 96-well plate and allowed to adhere for 24 h. After the cells were further treated with the indicated concentrations of Xn or DMSO (control) for 24 h, the medium was removed and replaced with fresh medium containing 600 μM H_2O_2 for 12 h or 200 μM 6-OHDA for 24 h. At the end of the treatments, 10 μL of MTT (5 mg/mL) was added to each well followed by incubation for an additional 4 h at 37 °C. An extraction buffer (100 μL, 10% SDS, 5% isobutanol, 0.1% HCl) was added, and the cells were incubated overnight at 37 °C. The absorbance was measured at 570 nm using a microplate reader (Thermo Scientific Multiskan GO, Finland).

Lactate Dehydrogenase (LDH) Release Assay. PC12 cells were seeded in 12-well plates at a density of 2×10^5 cells/well. On the following day, the cells were exposed to various concentrations of Xn for 24 h, followed by addition of 600 μM H_2O_2 for an additional 12 h or 200 μM 6-OHDA for an additional 24 h. The leakage of LDH from cultured cells was quantified by measuring LDH activity in the culture medium. Briefly, 50 μL of the culture medium was mixed with 110 μL of 100 mM Tris−HCl buffer (pH 7.4), 20 μL of 2 mM NADH, and 20 μL of 20 mM pyruvate, and the change of absorbance at 340 nm due to the consumption of NADH was monitored every 20 s for 5 min. The content of LDH release was calculated by normalizing the LDH activity of samples to that measured in culture medium from the control cells.

Hoechst 33342 Staining. PC12 cells were plated in 12-well plates at a density of 2×10^5 cells/well. On the following day, the cells were incubated with the indicated concentrations of Xn for 24 h. After replacement with the fresh medium containing 600 μM H_2O_2 or 200 μM 6-OHDA, the cells were allowed to continue growing for 12 h (H_2O_2) or for 24 h (6-OHDA). After the treatments, Hoechst 33342 was subsequently added to a final concentration of 5 μg/mL to stain the nuclei. The cells were visualized and photographed with a Leica inverted fluorescent microscope.

Measurement of Caspase-3 Activity. PC12 cells were seeded in 60 mm dishes at a density of 2×10^6 cells/well for 24 h and then treated with different concentrations of Xn or DMSO for another 24 h. After replacement with the fresh medium containing 600 μM H_2O_2 or 200 μM 6-OHDA for 24 h, the cells were harvested, washed with PBS, and lysed with RIPA buffer (50 mM Tris−HC,l pH 7.5, 2 mM EDTA, 0.5% deoxycholate, 150 mM NaCl, 1% Triton X-100, 0.1% SDS, 1 mM

DOI: 10.1021/jf505075n
J. Agric. Food Chem. XXXX, XXX, XXX−XXX

Na_3VO_4, and 1 mM PMSF) for 30 min on ice. The protein concentration was quantified using the Bradford procedure. A cell extract containing 15 μg of total proteins was incubated with the assay mixture (50 mM Hepes, 2 mM EDTA, 5% glycerol, 10 mM DTT, 0.1% CHAPS, 0.2 mM Ac-DEVD-pNA, pH 7.5) for 4 h at 37 °C in a final volume of 100 μL. The absorbance at 405 nm was measured using a microplate reader. The caspase-3 activity was expressed as the percentage of the control cells that grow with DMSO treatment.

Assessment of the Intracellular ROS. PC12 cells (2×10^5 cells/well) were seeded into 12-well plates and allowed to adhere for 24 h. Then the cells were treated with Xn or DMSO for another 24 h, followed by replacement with the fresh medium containing 600 μM H_2O_2 for 3 h or 200 μM 6-OHDA for 6 h. After removal of the culture medium, the ROS indicator DCFH-DA (10 μM) in fresh FBS-free medium was added to each well, and incubation was continued for 30 min at 37 °C in the dark. The cells were visualized and photographed under a fluorescent microscope. Intracellular ROS were quantified in PC12 cells using the green fluorescent probe DCFH-DA. Cells were seeded at 1×10^4 cells/well in black 96-well plates for 1 d. The cells were exposed to 600 μM H_2O_2 for 3 h or 200 μM 6-OHDA for 6 h after a 24 h pretreatment with or without Xn. After removal of the medium and staining of the cells with DCFH-DA (10 μM) for 30 min, the cells were washed with PBS and the fluorescence intensity at 525 nm excited at 488 nm in each well was read by an Infinite M200 (Tecan). The ROS levels are expressed as the percentage of treated cells compared to the control.

Real-Time Reverse Transcription PCR (RT-PCR). PC12 cells were seeded in 60 mm dishes at a density of 2×10^6 cells/well for 24 h, followed by treatment with 0.5 μM Xn for 0, 6, and 12 h. As a positive control, the cells were treated with tBHQ (20 μM) for 6 h. For the injury models, the cells were further exposed to 600 μM H_2O_2 for 6 h or 200 μM 6-OHDA for 12 h after the cells were pretreated with Xn for 6 h. Total RNA was isolated from cells using an RNAiso Plus (TaKaRa, Dalian, China) according to the manufacture's protocol and quantified through 260 nm/280 nm wavelength measurement. Reverse transcription was performed using a Primescript RT reagent kit according to the manufacture's protocol (TaKaRa). RT-PCR was performed on an Agilent Technologies Stratagene Mx3005P RT-PCR system using SYBR Premix Ex Taq II (Tli RNaseH Plus). PCR primers specific to each gene were as follows: glyceraldehyde-3-phosphate dehydrogenase (GAPDH), 5′-cagtgccagcctcgtctcat-3′ (forward, F) and 5′-aggggccatccacagtcttc-3′ (reverse, R); heme oxygenase 1 (HO-1), 5′-gccctggaagaggagatagag-3′ (F) and 5′-tagtgctgtgtggct-ggtgt-3′ (R); NAD(P)H:quinone oxidoreductase 1 (NQO1), 5′-tcaccactctactttgctccaa-3′ (F) and 5′-ttttctgctcctcttgaacctc-3′ (R); thioredoxin 1 (Trx1), 5′-ccttctttcattccctctgtgac-3′ (F) and 5′-cccaa-ccttttgaccctttttat-3′ (R); thioredoxin reductase 1 (TrxR1), 5′-actgc-tcaatccacaaacagc-3′ (F) and 5′-ccacggtctctaagccaatagt-3′ (R); catalytic subunit of glutamate−cysteine ligase (GCLC), 5′-caaggacaagaacac-accatct-3′ (F) and 5′-cagcactcaaagccataacaat-3′ (R); modifier subunit of glutamate−cysteine ligase (GCLM), 5′-ggcacaggtaaaacccaatagt-3′ (F) and 5′-ttcaatgtcagggatgctttct-3′ (R). The GAPDH was used as an internal control. Target gene expression was measured and was normalized to the GAPDH expression level.

Measurement of Total Glutathione. Quantification of the total glutathione was based on the enzymatic recycling method.[31] PC12 cells were seeded in 60 mm dishes at a density of 2×10^6 cells/well for 24 h and treated with different concentrations of Xn or vehicle for 24 h. For each sample, cells were collected and resuspended using ice-cold extraction buffer containing 0.1% Triton X-100 and 0.6% sulfosalicyclic acid in 0.1 M potassium phosphate buffer with 5 mM EDTA disodium salt, pH 7.5 (KPE buffer) . The cell suspension was sonicated in ice every 30 s for 2−3 min. After the cell suspension was centrifuged at 3000*g* for 4 min at 4 °C, the supernatant was immediately transferred to a new Eppendorf tube. A 120 μL solution containing 0.33 mg/mL DTNB and 1.66 units/mL glutathione reductase was added to each sample (20 μL). β-NADPH (60 μL, 0.66 mg/mL) was then added quickly, and the absorbance at 412 nm was measured every 15 s for 2 min. The same amounts of DMSO were added to the control experiments, and the activity is expressed as a percentage of the control.

Measurement of NQO1 Activity. The NQO1 activity was determined spectrophotometrically by monitoring the reduction of the electron acceptor 2,6-DCPIP at 600 nm.[27] In brief, PC12 cells were seeded in 60 mm dishes at a density of 2×10^6 cells/well for 24 h and treated with different concentrations of Xn or DMSO for another 24 h. The cells were harvested and lysed in RIPA buffer. The total protein concentration was quantified using the Bradford procedure. The enzymatic reaction was initiated by the addition of cell lysate (5 μg of total protein) to the reaction mixture (2 mM Tris−HCl, pH 7.4, 200 μM NADH, and 40 μM DCPIP), and the decrease in absorbance at 600 nm was measured every 15 s for 2 min at room temperature in the presence or absence of 20 μM dicoumarol, a known NQO1 inhibitor. The dicoumarol-inhibitable part of DCPIP's reduction was used to calculate the NQO1 activity. The same amounts of DMSO were added to the control experiments, and the activity is expressed as a percentage of the control.

Determination of Trx and TrxR Activity. After PC12 cells were treated with different concentrations of Xn for 24 h, the cells were harvested and washed twice with PBS. Total cellular proteins were extracted by RIPA buffer for 30 min on ice. The total protein content was quantified using the Bradford procedure. Trx and TrxR activity in cell lysates was measured by the end point insulin reduction assay.[32] Briefly, the cell extract containing 20 μg of total proteins was incubated in a final reaction volume of 50 μL containing 100 mM Tris−HCl (pH 7.6), 0.3 mM insulin, 660 μM NADPH, 3 mM EDTA, and 15 μM *E. coli* Trx (for assaying the activity of TrxR) or 250 nM recombinant rat TrxR1 (for assaying the activity of Trx) for 30 min at 37 °C. The reaction was terminated by adding 200 μL of 1 mM DTNB in 6 M guanidine hydrochloride, pH 8.0. A blank sample, containing everything except TrxR or Trx, was treated in the same manner. The absorbance at 412 nm was measured, and the blank value was subtracted from the corresponding absorbance value of the sample. The same amounts of DMSO were added to the control experiments, and the activity is expressed as a percentage of the control.

Western Blot Analysis. PC12 cells (4×10^6 cells/well) seeded in 100 mm dishes for 1 d and subsequently treated with Xn (0.5 μM) for 0, 2, 4, 6, 8 h were harvested, and different cell extracts were prepared according to the published procedure.[27] For the whole cell protein extraction, PC12 cells were washed with ice-cold PBS three times and then with RIPA buffer for 30 min on ice. Cell lysates were centrifuged at 12000*g* for 20 min at 4 °C, and the supernatant was collected for analysis or stored at −80 °C.

For the cytosolic and nuclear extracts, the cells were rinsed with ice-cold PBS, and the pellet was dissolved in 100 μL of buffer A (10 mM Hepes, pH 7.9, 10 mM KCl, 0.1 mM EDTA, 0.1 mM EGTA, 1 μM DTT, and 1 μM protease inhibitor cocktail freshly added to buffer A). After 15 min of incubation, 10 μL of Nonidet-P40 (10%) was added, and the lysate was vortexed for 15 s. Thereafter, the lysate was repeatedly centrifuged for 10 min (1000*g*, 4 °C) to separate the nuclei from the cytosolic fraction. The supernatant (cytosolic fraction) was stored on ice. The pellet was resuspended in 100 μL of buffer B (20 mM Hepes, pH 7.9, 0.4 M NaCl, 1 mM EDTA, 1 mM EGTA, 1 μM DTT, and 1 μM protease inhibitor cocktail freshly added to buffer B) and incubated on ice for 15 min with vortexing for 10−15 s every 2 min. After a final centrifugation step for 10 min (20000*g*, 4 °C), the supernatant (nuclear extract) and the cytosolic extract were used for analysis or stored at −80 °C. For Western blot analysis, equal amounts of protein in each lysate sample were separated by SDS−PAGE and electroblotted onto a PVDF membrane (Millipore, United States). After blocking with 2.5% nonfat milk at room temperature for 2 h, the membranes were incubated with primary antibodies at 4 °C overnight. The membranes were washed with TBST three times and then incubated with horseradish peroxidase-conjugated secondary antibodies at room temperature for 1 h. The signal was detected using an enhanced chemiluminescence (ECL) kit from GE Healthcare. The band intensity was quantified by Image Pro Plus 6.0

Generation of Nrf2-Knockdown PC12 Cells Using Short Hairpin RNAs. The short hairpin RNAs specifically targeting the rat

DOI: 10.1021/jf505075n
J. Agric. Food Chem. XXXX, XXX, XXX−XXX

Scheme 1. Synthesis of Xn and TH-Xn

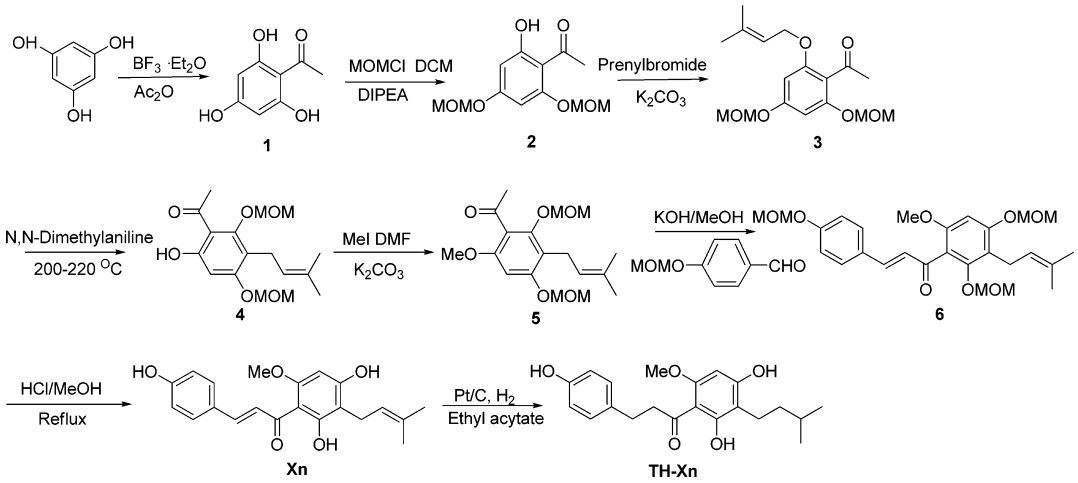

Nrf2 gene (shNrf2) and with a scrambled sequence (shNT) as the control were used for Nrf2-knockdown experiments.[27] The exponentially growing PC12 cells were transfected with different shRNAs using GeneTran III transfection reagent according to the manufacture's instructions. After 48 h of transfection, the cells were maintained in DMEM, 10% FBS, 2 mM glutamine, and 100 units/mL penicillin/streptomycin at 37 °C in a humidified atmosphere of 5% CO_2 and selected by supplementation with 0.5 mg/mL G418. Knockdown of the Nrf2 expression in the cells was analyzed by Western blotting.

Statistics. Data are presented as the mean ± SE. Statistical differences between two groups were assessed by Student's *t* test. Comparisons among multiple groups were performed using one-way analysis of variance (ANOVA), followed by a post hoc Scheffe test. $P < 0.05$ was used as the criterion for statistical significance.

RESULTS AND DISCUSSION

Chemical Synthesis. Xn and TH-Xn described in this study were prepared according to the published procedures.[30,33] The synthetic routes are illustrated in Scheme 1 and afforded a total yield of 5.0% in seven steps. Analysis of the chemical structure of Xn reveals it belongs to chalcones, the structure of which could be easily constructed by the base-catalyzed Claisen−Schmidt condensation of an aldehyde and ketone in a polar solvent such as ethanol or methanol. The key intermediate **4** was prepared from **3** via para-Claisen rearrangement. The skeleton of Xn was afforded by reaction of **5** with *p*-hydroxybenzaldehyde employing KOH as a catalyst in anhydrous methanol. Removal of the methoxymethyl protecting groups under acidic conditions furnishes the desired Xn. TH-Xn was prepared by the Pt/C-catalyzed hydrogenation of Xn. Xn and TH-Xn were fully characterized by ^{1}H and ^{13}C NMR and MS (Figures S2−S6 in the Supporting Information). The detailed chemical syntheses are described in the Supporting Information. The stability of Xn was determined in DMEM cell culture medium by scanning its absorbance spectra, and >90% of the compound remained after 6 h (Figure S1, Supporting Information).

Scavenging Free Radicals in Vitro. Xn is a polyphenol, and thus, we first investigated its antioxidant activity in vitro. ABTS radical cation is a stable radical with a characteristic absorbance at 734 nm. Neutralization of ABTS free radicals could be easily determined by following the decrease of optical density at 734 nm. As shown in Figure 1A, Xn displays moderate efficiency to scavenge ABTS free radicals. We also employed a model of free-radical-mediated lipid peroxidation to assay the antioxidant activity of Xn. Thermal decomposition of AAPH in aqueous solution under aerobic conditions constantly generates peroxyl radicals, which attack membrane unsaturated lipids to induce lipid peroxidation. Xn remarkably protects the erythrocyte ghost from AAPH-induced formation of TBARS (Figure 1B), a biomarker of lipid peroxidation. Taken together, Xn could directly scavenge free radicals in vitro.

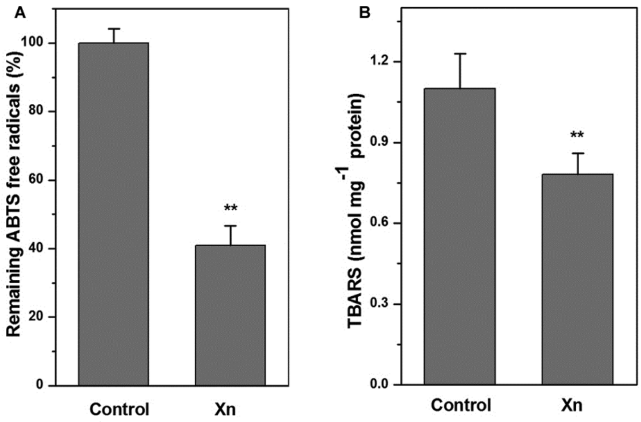

Figure 1. Scavenging of free radicals by Xn in vitro. (A) Neutralization of ABTS free radicals by Xn. (B) Prevention of the free-radical-mediated formation of TBARS in erythrocyte ghost by Xn. Key: **, $P < 0.01$ vs the control group.

Protecting PC12 Cells from H_2O_2- and 6-OHDA-Induced Damage. As Xn was reported to have cytotoxicity,[16,18] we first determined this effect in PC12 cells. Xn shows little cytotoxicity toward PC12 cells at submicromolar concentrations, and significant cytotoxicity was observed only at concentrations greater than 2 μM (Figure 2A). Thus, the concentrations of Xn used in the following protection experiments are no more than 1 μM. Next, we asked if Xn has cytoprotection at nontoxic concentrations in PC12 cells. Hydrogen peroxide, an endogenous cellular signaling molecule, has been extensively used as an inducer of oxidative stress in many cellular models. As shown in Figure 2B, PC12 cells treated with H_2O_2 only showed about 50% cell death compared with the control group. However, if the cells were pretreated with Xn (0.5 μM) for 24 h followed by H_2O_2 insult, the population of viable cells increased to about 75%. This protection was significant even at 0.1 μM Xn. 6-OHDA is a

DOI: 10.1021/jf505075n
J. Agric. Food Chem. XXXX, XXX, XXX−XXX

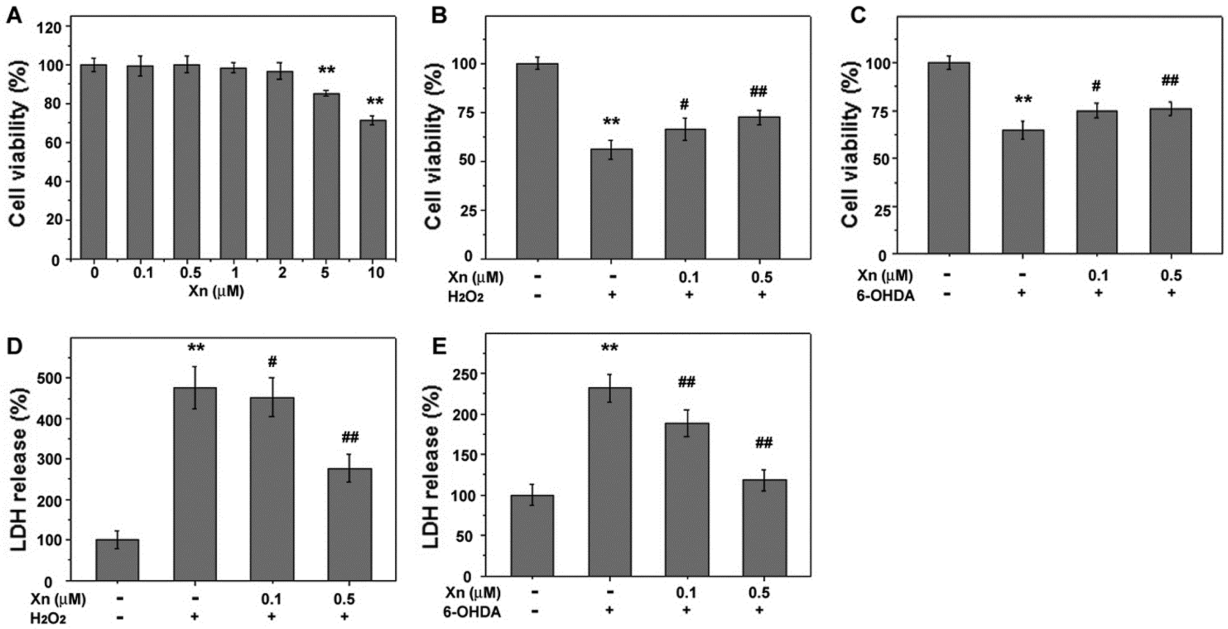

Figure 2. Protection of Xn against H_2O_2- or 6-OHDA-induced PC12 cell damage. (A) Cytotoxicity evaluation of Xn toward PC12 cells. The cells were treated with the indicated concentrations of Xn for 24 h, and the cytotoxicity of Xn was determined by the MTT assay. Protection against (B) H_2O_2-induced and (C) 6-OHDA-induced PC12 cell damage. PC12 cells (1×10^4 cells/well) were plated in a 96-well plate for 1 d and subsequently treated with Xn for another 24 h. After replacement with the fresh medium containing H_2O_2 and 6-OHDA and after incubation was continued for the indicated times, the cell viability was measured by MTT assay. The content of LDH in the medium after H_2O_2 (D) or 6-OHDA (E) treatment was determined as described in the Materials and Methods. All data represent the means ± SE of three independent experiments. Key: **, $P < 0.01$ vs the vehicle group; #, $P < 0.05$ vs the H_2O_2- or 6-OHDA-treated group; ##, $P < 0.01$ vs the H_2O_2- or 6-OHDA-treated group.

potent neurotoxin and is widely used to generate an experimental model of Parkinson's disease. 6-OHDA-mediated neurotoxicity is engendered, at least in part, by its ability to generate ROS.[34] As shown in Figure 2C, 6-OHDA treatment reduced cell viability to about 60% of that of the control. Similarly, addition of Xn, at either 0.1 or 0.5 μM, also markedly promoted cell viability to more than 75%. Lactate dehydrogenase (LDH) is a soluble cytosolic enzyme that is released into the culture medium following loss of membrane integrity resulting from cell damage. To confirm the cytoprotection of Xn, we further determined the content of LDH leakage after H_2O_2 or 6-OHDA insult. As shown in Figure 2D,E, H_2O_2 and 6-OHDA cause ~4.7-fold and ~2.4-fold increases of LDH release, respectively. Pretreatment of PC12 cells with Xn significantly reduces the leakage of LDH in a dose-dependent manner. Taken together, Xn at nontoxic concentration can significantly protect PC12 cells from H_2O_2- or 6-OHDA-induced cell damage.

Alleviating H_2O_2- and 6-OHDA-Induced PC12 Cell Apoptosis. Nuclear condensation and caspase-3 activation are hallmarks of cell apoptosis. The morphologic changes of the nuclei were revealed by Hoechst staining. As shown in Figure 3A,B, both H_2O_2 and 6-OHDA elicit apoptosis in PC12 cells evidenced by the appearance of apoptotic nuclei as highly fluorescent, condensed bodies (indicated by arrows), while no apparent apoptotic nuclei were observed in control cells. Pretreatment of PC12 cells with nontoxic concentrations of Xn remarkably lowers the population of apoptotic nuclei. Activation of caspase-3 is a biochemical character in all apoptotic cells. We thus further quantified the level of caspase-3 activation. Both H_2O_2 and 6-OHDA activate the cellular caspase-3, but with different potencies (Figure 3C,D). Again, Xn significantly alleviates the extent of caspase-3 activation in a concentration-dependent manner. Collectively, Xn alleviates H_2O_2- and 6-OHDA-induced apoptotic cell death in PC12 cells.

Preventing ROS Accumulation in PC12 Cells. DCFH-DA is a cell-permeable, nonfluorescent probe. After diffusing into cells, DCFH-DA is deacetylated by cellular esterases to nonfluorescent 2′,7′-dichlorodihydrofluorescin (DCFH), which is rapidly converted to highly fluorescent 2′,7′-dichlorofluorescein (DCF) upon reacting with ROS. Stimulation of the cells with H_2O_2 or 6-OHDA leads to intracellular burst of ROS, while the control cells display a negligible ROS level, as revealed by DCFH-DA staining (Figure 4A,B), and the quantifying results are shown in Figure 4C,D. Pretreatment of the cells with Xn remarkably reduces the ROS accumulation induced by either H_2O_2 or 6-OHDA. As oxidative stress, arising from the overproduction of ROS beyond the cellular capacity to remove them, has been implicated in a common pathway of neurotoxicity in a wide variety of acute and chronic neurologic disorders, the inhibition of ROS accumulation in neuronal cells might be the molecular basis of the neuroprotective action of Xn.

Inducing Phase II Gene Expression. Xn belongs to the chalcone family, which bears an α,β-unsaturated ketone structure. Due to the electron-deficient character of the double bond, this structure is renowned as a Michael acceptor moiety, which is a core structure of many reported small-molecule ARE inducers.[7] In analogy to known ARE activators, we thus hypothesized that Xn might activate the cellular ARE response. We measured the expression of Nrf2-driven antioxidant/detoxifying genes (HO-1, NQO1, Trx1, TrxR1, GCLC, and GCLM) at 0, 6, and 12 h after treatment with Xn (0.5 μM) in PC12 cells (Figure 5). Although the positive control tBHQ displays more potency, the induction of these genes by Xn is

DOI: 10.1021/jf505075n
J. Agric. Food Chem. XXXX, XXX, XXX−XXX

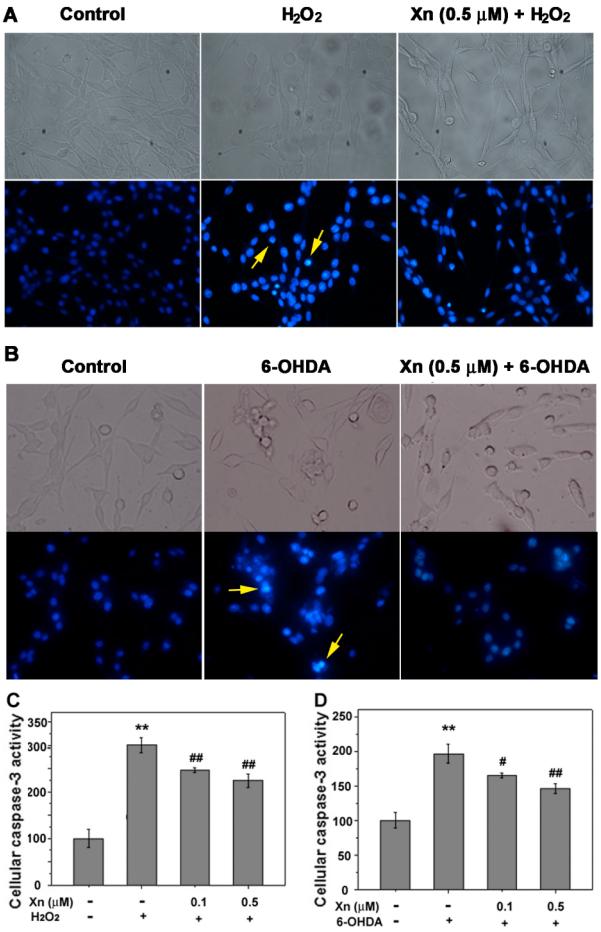

Figure 3. Inhibition of H_2O_2- or 6-OHDA-induced apoptosis in PC12 cells. PC12 cells were treated as described in the Materials and Methods, and the morphological changes of the nuclei were determined by Hoechst 33342 staining (A, B). Activation of the cellular caspase-3 (C, D) was determined by a colorimetric assay as described in the Materials and Methods. The data represent the means ± SE of three independent experiments. Key: **, $P < 0.01$ vs the vehicle group; #, $P < 0.05$ vs the H_2O_2- or 6-OHDA-treated group; ##, $P < 0.01$ vs the H_2O_2- or 6-OHDA-treated group.

significant. The time-course studies showed the highest induction of the genes at 6 h after stimulation with Xn. The HO-1 and TrxR1 mRNAs were highly transcribed by ∼2.8- and 2.3-fold increases, respectively, after treatment with Xn for 6 h. The induction of other genes is moderate but sustainable, and this induction could last for 12 h. The phase II genes were also induced if the cells were pretreated with Xn followed by the oxidant insults. Our data suggest that Xn treatment can effectively promote the transcription of Nrf2-driven antioxidant/detoxifying genes.

Upregulating the Antioxidant Defense System in PC12 Cells. The induction of phase II enzymes is an important defense mechanism against exogenous stress. As a series of phase II genes have been upregulated at different levels, we then examined the corresponding gene products. Xn dose-dependently elevated HO-1, NQO1, TrxR1, and Trx1 protein expression (Figure 6). The glutamate cysteine ligase, composed of a GCLC and a GCLM subunit, is a rate-limiting enzyme for cellular GSH synthesis. As a consequence of the elevation of GCLC gene expression, the total GSH level in PC12 cells was increased by ∼1.6-fold (Figure 6C). By adopting the

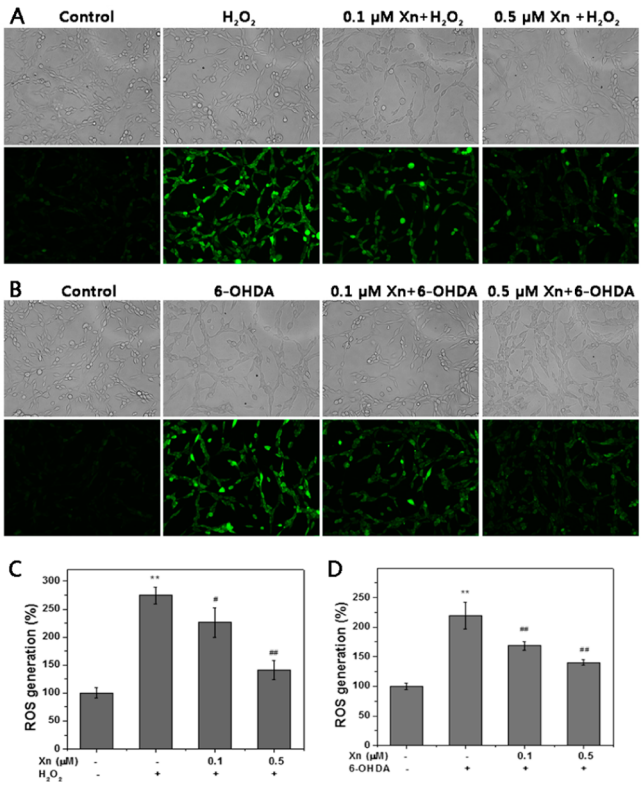

Figure 4. Prevention of ROS accumulation in PC12 cells by Xn. Pretreatment of the cells with Xn significantly alleviates ROS accumulation induced by H_2O_2 (A, C) or 6-OHDA (B, D) determined by DCFH-DA staining as described in the Materials and Methods. The fluorescence images (A, B) were acquired by inverted fluorescence microscopy. The ROS level was quantified in (C) and (D) by a fluorescence microplate reader, Infinite M200 (Tecan). Key: **, $P < 0.01$ vs the vehicle group; #, $P < 0.05$ vs the H_2O_2- or 6-OHDA-treated group; ##, $P < 0.01$ vs the H_2O_2- or 6-OHDA-treated group.

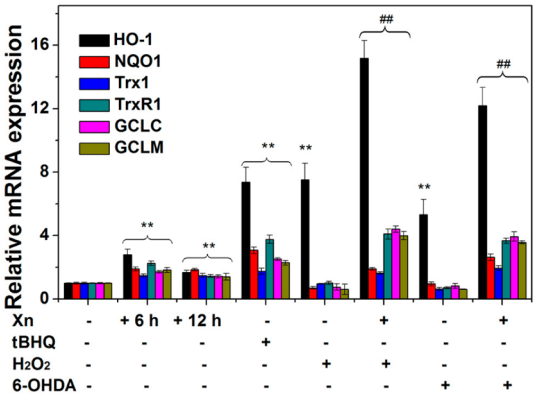

Figure 5. Induction of cytoprotective genes in PC12 cells by Xn. The cells were treated, and the mRNA levels of different genes were analyzed and normalized using GAPDH as an internal standard by qRT-PCR as described in the Materials and Methods. Pretreatment of the cells with Xn significantly elevates phase II gene expression under H_2O_2 or 6-OHDA conditions determined by qRT-PCR. PC12 cells were pretreated with Xn for 6 h or cotreated with H_2O_2 or 6-OHDA for another 6 or 12 h. tBHQ was used as a positive control. The data represent the means ± SE of three independent experiments. Key: *, $P < 0.05$ vs the control group (0 h); **, $P < 0.01$ vs the control group (0 h); #, $P < 0.05$ vs the H_2O_2- or 6-OHDA-treated group; ##, $P < 0.01$ vs the H_2O_2- or 6-OHDA-treated group.

DOI: 10.1021/jf505075n
J. Agric. Food Chem. XXXX, XXX, XXX−XXX

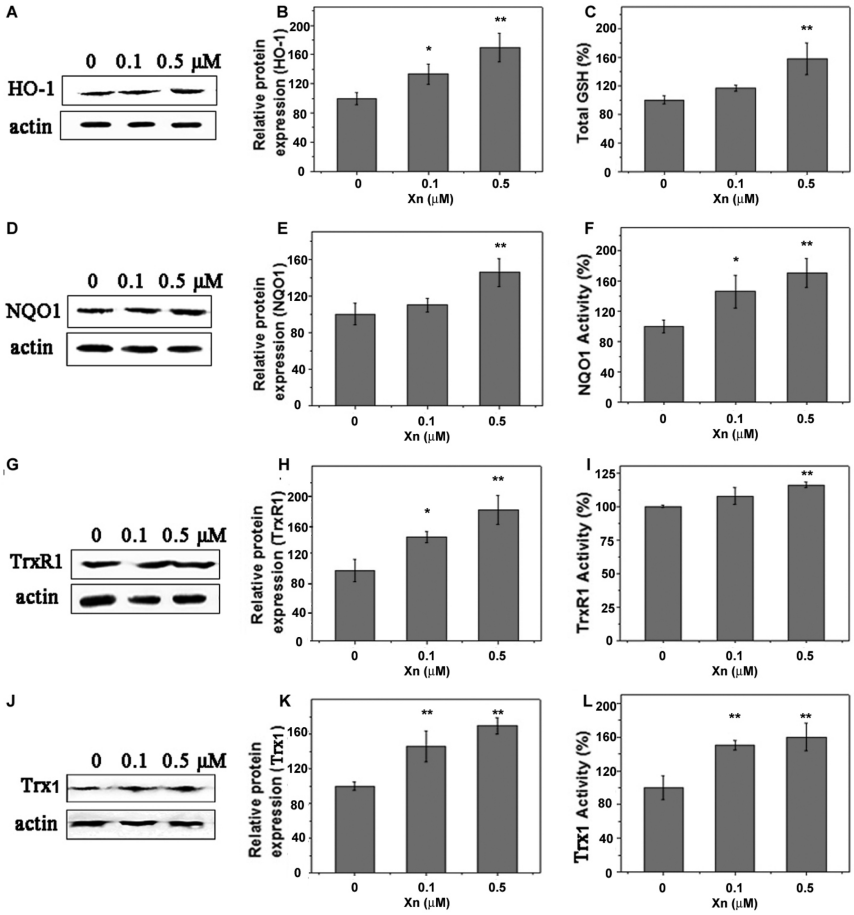

Figure 6. Upregulation of antioxidant enzymes by Xn in PC12 cells. (A) Induction of HO-1 protein expression by Xn. (B) Quantification of the band intensity in (A). (C) Xn induces upregulation of GSH in PC12 cells. The total intracellular GSH was measured as described in the Materials and Methods. Induction of NQO1 expression (D) and enzyme activity (F) by Xn. (E) Quantification of the band intensity in (D). Induction of TrxR1 expression (G) and total TrxR1 enzyme activity (I) by Xn. (H) Quantification of the band intensity in (G). Induction of Trx1 protein expression (J) and total Trx enzyme activity (L) by Xn. (K) Quantification of the band intensity in (J). Data are expressed as the means ± SE of three experiments. Key: *, $P < 0.05$ vs the vehicle group; **, $P < 0.01$ vs the vehicle group.

convenient assays, we further determined the cellular activity of NQO1, TrxR1, and Trx1. In line with the upregulation of protein expression, all the enzymes' activities were significantly increased (Figure 6F,I,L). After Xn (0.5 μM) treatment, the NQO1 activity (Figure 6F), TrxR1 activity (Figure 6I), and Trx1 activity (Figure 6L) were increased by ∼1.7-, ∼1.2-, and ∼1.5-fold, respectively. Our data demonstrate that Xn at submicromolar concentration could efficiently boost various endogenous cytoprotective molecules.

Promoting Nrf2 Nuclear Localization. Induction of antioxidant gene expression via the Nrf2-dependent cytoprotective pathway requires translocation of Nrf2 from the cytosol to the nucleus. We therefore examined whether Xn could promote Nrf2 to accumulate in the nuclei. After isolation of the nuclei from the cells, the total Nrf2, the cytosolic Nrf2, and the nuclear Nrf2 were determined by immunoblots. Upon Xn treatment, immunoblotting results revealed that the total Nrf2 expression increased, peaking at 4 h, and decreased to the basal level at 8 h (Figure 7A). Notably, the cytosolic Nrf2 decreased gradually, coincident with its continuous accumulation in the nuclei (Figure 7B,C), indicating the translocation of Nrf2 from the cytosol to the nuclei. We also analyzed the change of nuclear Nrf2 under H_2O_2 or 6-OHDA treatment conditions. As shown in Figure 7D, H_2O_2 or 6-OHDA alone has a marginal effect on the Nrf2 nuclear accumulation. However, after pretreatment with Xn followed by the oxidant insult, the amount of Nrf2 in the nucleus remarkably increased. The presence of Nrf2 in the nuclei would facilitate its binding to ARE and thus subsequently initiates the transcription process to induce the phase II gene expression.

Requiring the α,β-Unsaturated Ketone Structure in Xn and Nrf2 for Cytoprotection. As aforementioned, we speculated that the α,β-unsaturated ketone moiety in Xn and the transcription factor Nrf2 are key determinants for the action of Xn in PC12 cells. We prepared TH-Xn, a molecule without the α,β-unsaturated ketone structure, and generated Nrf2-knockdown PC12 cells to validate the molecular mechanism underlying the cytoprotection of Xn. Hydrogenation of Xn to TH-Xn almost completely abolishes the protective effect (Figure 8A), indicating the importance of the α,β-unsaturated ketone structure in Xn. Next, we compared the protection of Xn in PC12 cells with different Nrf2 expressions. After confirmation of the knockdown efficiency of Nrf2 (Figure 8B), we evaluated the effect of Xn against oxidative insult toward different cells. As shown in Figure 8C,D, Xn displays a protective pattern in PC12 cells transfected with shNT similar to that observed in wild-type PC12 cells. However, this protection is drastically lost in PC12 cells transfected with

DOI: 10.1021/jf505075n
J. Agric. Food Chem. XXXX, XXX, XXX−XXX

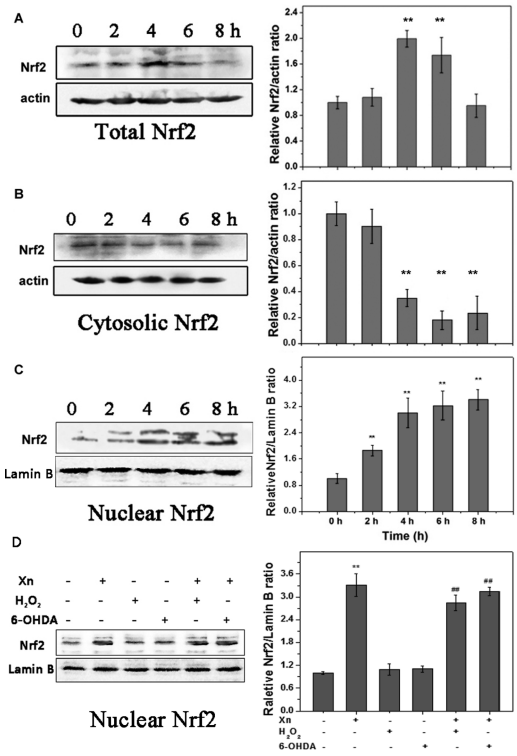

Figure 7. Promotion of Nrf2 nuclear accumulation by Xn. After the cells were treated with Xn (0.5 μM) for 0, 2, 4, 6, and 8 h, they were harvested, and different cell extracts were prepared as described in the Materials and Methods. The total Nrf2 (A), cytosolic Nrf2 (B), and nuclear Nrf2 (C) were analyzed by Western blotting. (D) Pretreatment of the cells with Xn promotes nuclear Nrf2 accumulation under H_2O_2 or 6-OHDA treatment conditions. PC12 cells were pretreated with Xn for 6 h and cotreated with H_2O_2 or 6-OHDA for another 6 or 12 h. Actin or lamin B was used as a loading control. Quantification of the blots is presented in the right panel. The data are expressed as the means ± SE of three experiments. Key: *, $P < 0.05$ vs the control group (0 h); **, $P < 0.01$ vs the control group (0 h). #, $P < 0.05$ vs the H_2O_2- or 6-OHDA-treated group; ##, $P < 0.01$ vs the H_2O_2- or 6-OHDA-treated group.

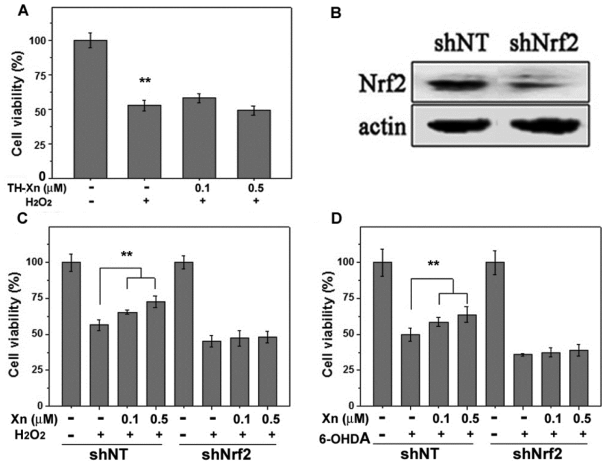

Figure 8. Involvement of Nrf2 in the cytoprotection of Xn in PC12 cells. (A) Protection of TH-Xn against H_2O_2-induced PC12 cell damage. (B) Evaluation of Nrf2-knockdown efficiency by different shRNAs. PC12 cells were transfected with shRNAs specifically targeting the rat Nrf2 gene (shNrf2s) or nontargeting shRNA (shNT), and the efficiency of silencing Nrf2 was evaluated by Western blots. (C, D) Impairment of cytoprotection of Xn in Nrf2-knockdown cells. Different PC12 cells were treated with Xn for 24 h followed by treatment with 600 μM H_2O_2 for 12 h or 200 μM 6-OHDA for 24 h. The cell viability was determined by MTT assay. The results are expressed as the means ± SE. Key: **, $P < 0.01$; *, $P < 0.05$.

shNrf2 (Figure 8C,D), demonstrating the definite involvement of Nrf2 in cytoprotection of Xn in PC12 cells.

Common targets and mechanisms of neurodegenerative diseases have been elegantly summarized in a recent paper.[35] Among various pathogenic hypotheses, increasing evidence has supported that oxidative stress is a causal, or at least an ancillary, factor in the progressive degeneration of a subset of neurons, which is the pathologic hallmark of adult-onset neurodegenerative diseases.[1,36] Surgical operation to replace the dying or dead neurons in these diseases has been demonstrated only with limited success.[37] Therefore, pharmacological management intended to assuage the oxidative stress is one promising strategy to protect loss of neurons, which is expected to eventually lead to retardation or blockage of the neurodegenerative progression. Tactics against oxidative stress include direct antioxidative action by supplying exogenous antioxidants and indirect defense by activating the pathway(s) involved in expression of endogenous cytoprotective molecules. In this regard, accumulating enthusiasm has been devoted to discovering and developing novel antioxidants or molecules that may prompt endogenous antioxidant defense as potential therapeutic agents for neurodegenerative disorders.[7]

Preceding studies have suggested that Xn could promote neuronal differentiation as well as neurite outgrowth[23] and prevent middle cerebral artery occlusion-induced cerebral ischemia in rats[38] to confer neuroprotective function. We revealed in this work for the first time that Xn displayed potent cytoprotection against H_2O_2- or 6-OHDA-mediated cell damage in PC12 cells via the induction of phase II antioxidant/detoxifying enzymes. Treatment of PC12 cells with Xn significantly upregulates a set of Nrf2-driven phase II genes as well as the corresponding gene products, including the antioxidant enzymes (HO-1, NQO1, Trx1, and TrxR1) and small peptide antioxidant GSH. Activation of Nrf2 by Xn in different types of cells, including microglial BV2 cells,[22] human hepatocytes,[39] and Hepa 1c1c7 cells,[40] and even in vivo,[41] has been reported. Besides, Xn has been demonstrated to possess diverse functions in a variety of cellular assays, such as anticancer[14−18] and anti-inflammation.[15,22] However, there has been no study on induction of Nrf2 in neuronal cells prior to this work, and most of the activity in these cellular assays requires higher concentrations of Xn (>1 μM). We demonstrated that Xn, as low as 0.1 μM, could significantly protect neuronal cells from oxidative insult. This concentration could be easily reached in vivo by daily intake of Xn-containing products, such as beers. The pharmacokinetics and metabolites of xanthohumol in rats have been evaluated by giving the rats intravenous injection or oral administration.[20,42] The highest plasma concentration of 2.97 mg/L (~8 μM) could be reached after intravenous injection at a dose of 1.86 mg/kg. Oral administration of Xn also leads to a significant amount of plasma circulation. One major challenge for most neuroprotective agents is their ability to pass through the blood−brain barrier (BBB). There are no available BBB penetration data for the flavonoid Xn. However, there is strong evidence showing that structurally different flavonoids are able to traverse the BBB.[43] The prenyl group further increases the

DOI: 10.1021/jf505075n
J. Agric. Food Chem. XXXX, XXX, XXX−XXX

lipophilicity of Xn, which favors BBB penetration. It is much like Xn having the ability to pass through the BBB in vivo. Thus, our finding, i.e., the induction of endogenous cytoprotective enzymes by Xn to confer potential neuroprotection, is of physiological significance.

The Keap1−Nrf2−ARE regulatory pathway plays a central role in protecting cells against oxidative or electrophilic insult. Under unstressed conditions, Nrf2 is bound to the repressor protein Keap1, which anchors Nrf2 in the cytoplasm and targets it for ubiquitination and proteasome degradation. Upon exposure to stressors, the Nrf2−Keap1 complex dissociates and Nrf2 translocates to the nucleus. The mechanisms underlying the activation of the Keap1−Nrf2−ARE pathway are not well understood but may involve oxidation/alkylation of key thiol(s) in Keap1 and/or phosphorylation of Nrf2. Upon exposure to electrophiles or oxidants, the Cys-rich protein Keap1 is modified by forming covalent adduct or disulfide bond(s) within the protein, and it is this Cys-based modification of Keap1 that allows dissociation of Nrf2 from Keap1 and subsequent nuclear translocation of Nrf2. Analysis of the chemical structure of Xn reveals that the molecule contains one α,β-unsaturated ketone moiety, a thiol-reactive electrophilic center that may covalently modify the Cys thiols. Many natural or synthetic molecules bearing such a structure are known effective inducers of phase II genes.[6,44] Thus, alkylation of certain Cys residue(s) might be the molecular basis for the activation of the Keap1−Nrf2−ARE pathway by Xn, which was evidenced by the liquid chromatography−tandem mass spectrometry analysis[40] and our observation that removal of the electrophilic center from Xn blocks such protection (Figure 8A). Abrogating the protection of Xn by silencing Nrf2 expression in PC12 cells further supports the involvement of Nrf2 in the cellular action of Xn. Our findings suggest a novel neuroprotective mechanism of Xn shown schematically in Figure 9. The lipophilic character of Xn allows it to easily penetrate the cell membrane and accumulate within cells. As a polyphenol, Xn could directly neutralize ROS. Furthermore, the α,β-unsaturated ketone structure in Xn allows it to bind covalently to the Cys residue(s) in the cytosolic inhibitory protein Keap1, thus breaking the Keap1−Nrf2 complex to prevent proteasome degradation of Nrf2 and release Nrf2. Subsequently, Nrf2 is translocated into the nucleus, where it binds to ARE and initiates the transcription of a variety of cytoprotective genes to confer protection against oxidative stress.

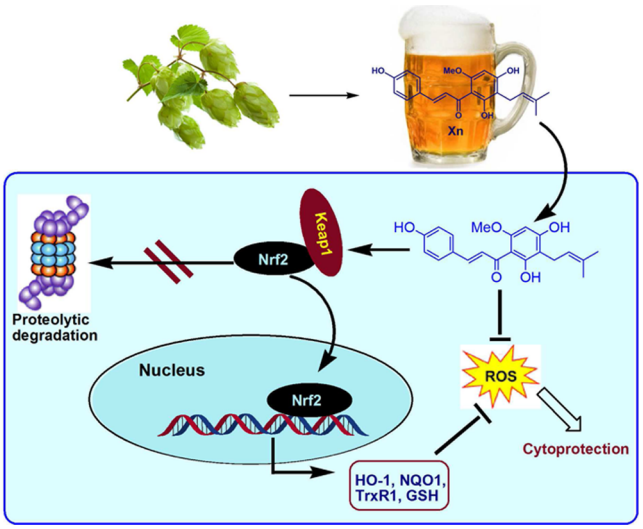

Figure 9. A neuroprotective mode of Xn in PC12 cells.

In summary, we conclude that Xn is effective in preventing oxidative-stress-induced neuronal cell damage. Xn displays a moderate capacity to directly neutralize ROS in vitro. More importantly, this cytoprotection is mediated by the induction of endogenous antioxidant defense molecules, which relies on the α,β-unsaturated ketone structure in Xn and the transcription factor Nrf2 in PC12 cells as removal of such a chemical structure or knockdown of Nrf2 abolishes the protection. Our discovery discloses that Xn is a novel small-molecule activator of the Keap1−Nrf2 pathway and provides deep insights into understanding the molecular mechanism underlying the cytoprotection of Xn. This mechanism of action could lead to the design and development of novel small molecules as potential neuroprotective agents.

■ ASSOCIATED CONTENT

Supporting Information

Stability of Xn determined by its absorbance spectrum and synthesis and original spectra of Xn and TH-Xn. This material is available free of charge via the Internet at http://pubs.acs.org.

■ AUTHOR INFORMATION

Corresponding Author

*E-mail: fangjg@lzu.edu.cn. Fax: +86 931 8915557.

Funding

Financial support from Lanzhou University (Fundamental Research Funds for the Central Universities, Grant lzujbky-2014-56) and Natural Science Foundation of Gansu Province (Grant 145RJZA225) is greatly acknowledged.

Notes

The authors declare no competing financial interest.

■ ACKNOWLEDGMENTS

We express heartfelt appreciation to Prof. Arne Holmgren for recombinant rat TrxR1 and *E. coli* Trx.

■ REFERENCES

(1) Halliwell, B.; Gutteridge, J. In *Free Radicals in Biology and Medicine*, 4th ed.; Oxford University Press: Oxford, U.K., 2007.

(2) Sauer, H.; Wartenberg, M.; Hescheler, J. Reactive oxygen species as intracellular messengers during cell growth and differentiation. *Cell Physiol. Biochem.* **2001**, *11*, 173−186.

(3) Barnham, K. J.; Masters, C. L.; Bush, A. I. Neurodegenerative diseases and oxidative stress. *Nat. Rev. Drug Discovery* **2004**, *3*, 205−214.

(4) Kobayashi, M.; Yamamoto, M. Nrf2-Keap1 regulation of cellular defense mechanisms against electrophiles and reactive oxygen species. *Adv. Enzyme Regul.* **2006**, *46*, 113−140.

(5) McMahon, M.; Itoh, K.; Yamamoto, M.; Hayes, J. D. Keap1-dependent proteasomal degradation of transcription factor Nrf2 contributes to the negative regulation of antioxidant response element-driven gene expression. *J. Biol. Chem.* **2003**, *278*, 21592−21600.

(6) Satoh, T.; McKercher, S. R.; Lipton, S. A. Nrf2/ARE-mediated antioxidant actions of pro-electrophilic drugs. *Free Radical Biol. Med.* **2013**, *65*, 645−657.

(7) Magesh, S.; Chen, Y.; Hu, L. Small molecule modulators of Keap1-Nrf2-ARE pathway as potential preventive and therapeutic agents. *Med. Res. Rev.* **2012**, *32*, 687−726.

DOI: 10.1021/jf505075n
J. Agric. Food Chem. XXXX, XXX, XXX−XXX

(8) Stevens, J. F.; Page, J. E. Xanthohumol and related prenylflavonoids from hops and beer: to your good health! *Phytochemistry* **2004**, *65*, 1317−1330.
(9) Stevens, J. F.; Taylor, A. W.; Deinzer, M. L. Quantitative analysis of xanthohumol and related prenylflavonoids in hops and beer by liquid chromatography-tandem mass spectrometry. *J. Chromatogr. A* **1999**, *832*, 97−107.
(10) Jain, M. G.; Hislop, G. T.; Howe, G. R.; Burch, J. D.; Ghadirian, P. Alcohol and other beverage use and prostate cancer risk among Canadian men. *Int. J. Cancer* **1998**, *78*, 707−711.
(11) Magalhaes, P. J.; Carvalho, D. O.; Cruz, J. M.; Guido, L. F.; Barros, A. A. Fundamentals and health benefits of xanthohumol, a natural product derived from hops and beer. *Nat. Prod. Commun.* **2009**, *4*, 591−610.
(12) Miranda, C. L.; Stevens, J. F.; Ivanov, V.; McCall, M.; Frei, B.; Deinzer, M. L.; Buhler, D. R. Antioxidant and prooxidant actions of prenylated and nonprenylated chalcones and flavanones in vitro. *J. Agric. Food Chem.* **2000**, *48*, 3876−3884.
(13) Doddapattar, P.; Radovic, B.; Patankar, J. V.; Obrowsky, S.; Jandl, K.; Nusshold, C.; Kolb, D.; Vujic, N.; Doshi, L.; Chandak, P. G.; Goeritzer, M.; Ahammer, H.; Hoefler, G.; Sattler, W.; Kratky, D. Xanthohumol ameliorates atherosclerotic plaque formation, hypercholesterolemia, and hepatic steatosis in ApoE-deficient mice. *Mol. Nutr. Food Res.* **2013**, *57*, 1718−1728.
(14) Harikumar, K. B.; Kunnumakkara, A. B.; Ahn, K. S.; Anand, P.; Krishnan, S.; Guha, S.; Aggarwal, B. B. Modification of the cysteine residues in IkappaBalpha kinase and NF-kappaB (p65) by xanthohumol leads to suppression of NF-kappaB-regulated gene products and potentiation of apoptosis in leukemia cells. *Blood* **2009**, *113*, 2003−2013.
(15) Monteiro, R.; Calhau, C.; Silva, A. O.; Pinheiro-Silva, S.; Guerreiro, S.; Gartner, F.; Azevedo, I.; Soares, R. Xanthohumol inhibits inflammatory factor production and angiogenesis in breast cancer xenografts. *J. Cell. Biochem.* **2008**, *104*, 1699−1707.
(16) Monteghirfo, S.; Tosetti, F.; Ambrosini, C.; Stigliani, S.; Pozzi, S.; Frassoni, F.; Fassina, G.; Soverini, S.; Albini, A.; Ferrari, N. Antileukemia effects of xanthohumol in Bcr/Abl-transformed cells involve nuclear factor-kappaB and p53 modulation. *Mol. Cancer Ther.* **2008**, *7*, 2692−2702.
(17) Gerhauser, C.; Alt, A.; Heiss, E.; Gamal-Eldeen, A.; Klimo, K.; Knauft, J.; Neumann, I.; Scherf, H. R.; Frank, N.; Bartsch, H.; Becker, H. Cancer chemopreventive activity of xanthohumol, a natural product derived from hop. *Mol. Cancer Ther.* **2002**, *1*, 959−969.
(18) Miranda, C. L.; Stevens, J. F.; Helmrich, A.; Henderson, M. C.; Rodriguez, R. J.; Yang, Y. H.; Deinzer, M. L.; Barnes, D. W.; Buhler, D. R. Antiproliferative and cytotoxic effects of prenylated flavonoids from hops (*Humulus lupulus*) in human cancer cell lines. *Food Chem. Toxicol.* **1999**, *37*, 271−285.
(19) Buckwold, V. E.; Wilson, R. J.; Nalca, A.; Beer, B. B.; Voss, T. G.; Turpin, J. A.; Buckheit, R. W., 3rd; Wei, J.; Wenzel-Mathers, M.; Walton, E. M.; Smith, R. J.; Pallansch, M.; Ward, P.; Wells, J.; Chuvala, L.; Sloane, S.; Paulman, R.; Russell, J.; Hartman, T.; Ptak, R. Antiviral activity of hop constituents against a series of DNA and RNA viruses. *Antiviral Res.* **2004**, *61*, 57−62.
(20) Legette, L. L.; Luna, A. Y.; Reed, R. L.; Miranda, C. L.; Bobe, G.; Proteau, R. R.; Stevens, J. F. Xanthohumol lowers body weight and fasting plasma glucose in obese male Zucker fa/fa rats. *Phytochemistry* **2013**, *91*, 236−241.
(21) Kirkwood, J. S.; Legette, L. L.; Miranda, C. L.; Jiang, Y.; Stevens, J. F. A metabolomics-driven elucidation of the anti-obesity mechanisms of xanthohumol. *J. Biol. Chem.* **2013**, *288*, 19000−19013.
(22) Lee, I. S.; Lim, J.; Gal, J.; Kang, J. C.; Kim, H. J.; Kang, B. Y.; Choi, H. J. Anti-inflammatory activity of xanthohumol involves heme oxygenase-1 induction via NRF2-ARE signaling in microglial BV2 cells. *Neurochem. Int.* **2011**, *58*, 153−160.
(23) Oberbauer, E.; Urmann, C.; Steffenhagen, C.; Bieler, L.; Brunner, D.; Furtner, T.; Humpel, C.; Baumer, B.; Bandtlow, C.; Couillard-Despres, S.; Rivera, F. J.; Riepl, H.; Aigner, L. Chroman-like cyclic prenylflavonoids promote neuronal differentiation and neurite outgrowth and are neuroprotective. *J. Nutr. Biochem.* **2013**, *24*, 1953−1962.
(24) Zhang, L.; Duan, D.; Cui, X.; Sun, J.; Fang, J. A selective and sensitive fluorescence probe for imaging endogenous zinc in living cells. *Tetrahedron* **2013**, *69*, 15−21.
(25) Duan, D.; Zhang, B.; Yao, J.; Liu, Y.; Sun, J.; Ge, C.; Peng, S.; Fang, J. Gambogic acid induces apoptosis in hepatocellular carcinoma SMMC-7721 cells by targeting cytosolic thioredoxin reductase. *Free Radical Biol. Med.* **2014**, *69*, 15−25.
(26) Duan, D.; Zhang, B.; Yao, J.; Liu, Y.; Fang, J. Shikonin targets cytosolic thioredoxin reductase to induce ROS-mediated apoptosis in human promyelocytic leukemia HL-60 cells. *Free Radical Biol. Med.* **2014**, *70*, 182−193.
(27) Yao, J.; Ge, C.; Duan, D.; Zhang, B.; Cui, X.; Peng, S.; Liu, Y.; Fang, J. Activation of the phase II enzymes for neuroprotection by ginger active constituent 6-dehydrogingerdione in PC12 cells. *J. Agric. Food Chem.* **2014**, *62*, 5507−5518.
(28) Liu, Y.; Duan, D.; Yao, J.; Zhang, B.; Peng, S.; Ma, H.; Song, Y.; Fang, J. Dithiaarsanes induce oxidative stress-mediated apoptosis in HL-60 cells by selectively targeting thioredoxin reductase. *J. Med. Chem.* **2014**, *57*, 5203−5211.
(29) Cai, W.; Zhang, L.; Song, Y.; Wang, B.; Zhang, B.; Cui, X.; Hu, G.; Liu, Y.; Wu, J.; Fang, J. Small molecule inhibitors of mammalian thioredoxin reductase. *Free Radical Biol. Med.* **2012**, *52*, 257−265.
(30) Cai, W.; Zhang, B.; Duan, D.; Wu, J.; Fang, J. Curcumin targeting the thioredoxin system elevates oxidative stress in HeLa cells. *Toxicol. Appl. Pharmacol.* **2012**, *262*, 341−348.
(31) Rahman, I.; Kode, A.; Biswas, S. K. Assay for quantitative determination of glutathione and glutathione disulfide levels using enzymatic recycling method. *Nat. Protoc.* **2006**, *1*, 3159−3165.
(32) Zhang, L.; Duan, D.; Liu, Y.; Ge, C.; Cui, X.; Sun, J.; Fang, J. Highly selective off-on fluorescent probe for imaging thioredoxin reductase in living cells. *J. Am. Chem. Soc.* **2014**, *136*, 226−233.
(33) Khupse, R. S.; Erhardt, P. W. Total synthesis of xanthohumol. *J. Nat. Prod.* **2007**, *70*, 1507−1509.
(34) Saito, Y.; Nishio, K.; Ogawa, Y.; Kinumi, T.; Yoshida, Y.; Masuo, Y.; Niki, E. Molecular mechanisms of 6-hydroxydopamine-induced cytotoxicity in PC12 cells: involvement of hydrogen peroxide-dependent and -independent action. *Free Radical Biol. Med.* **2007**, *42*, 675−685.
(35) Trippier, P. C.; Jansen Labby, K.; Hawker, D. D.; Mataka, J. J.; Silverman, R. B. Target- and mechanism-based therapeutics for neurodegenerative diseases: strength in numbers. *J. Med. Chem.* **2013**, *56*, 3121−3147.
(36) Klein, J. A.; Ackerman, S. L. Oxidative stress, cell cycle, and neurodegeneration. *J. Clin. Invest.* **2003**, *111*, 785−793.
(37) Freed, C. R.; Greene, P. E.; Breeze, R. E.; Tsai, W. Y.; DuMouchel, W.; Kao, R.; Dillon, S.; Winfield, H.; Culver, S.; Trojanowski, J. Q.; Eidelberg, D.; Fahn, S. Transplantation of embryonic dopamine neurons for severe Parkinson's disease. *N. Engl. J. Med.* **2001**, *344*, 710−719.
(38) Yen, T. L.; Hsu, C. K.; Lu, W. J.; Hsieh, C. Y.; Hsiao, G.; Chou, D. S.; Wu, G. J.; Sheu, J. R. Neuroprotective effects of xanthohumol, a prenylated flavonoid from hops (*Humulus lupulus*), in ischemic stroke of rats. *J. Agric. Food Chem.* **2012**, *60*, 1937−1944.
(39) Krajka-Kuzniak, V.; Paluszczak, J.; Baer-Dubowska, W. Xanthohumol induces phase II enzymes via Nrf2 in human hepatocytes in vitro. *Toxicol. Vitro* **2013**, *27*, 149−156.
(40) Dietz, B. M.; Kang, Y. H.; Liu, G.; Eggler, A. L.; Yao, P.; Chadwick, L. R.; Pauli, G. F.; Farnsworth, N. R.; Mesecar, A. D.; van Breemen, R. B.; Bolton, J. L. Xanthohumol isolated from *Humulus lupulus* inhibits menadione-induced DNA damage through induction of quinone reductase. *Chem. Res. Toxicol.* **2005**, *18*, 1296−1305.
(41) Dietz, B. M.; Hagos, G. K.; Eskra, J. N.; Wijewickrama, G. T.; Anderson, J. R.; Nikolic, D.; Guo, J.; Wright, B.; Chen, S. N.; Pauli, G. F.; van Breemen, R. B.; Bolton, J. L. Differential regulation of detoxification enzymes in hepatic and mammary tissue by hops (*Humulus lupulus*) in vitro and in vivo. *Mol. Nutr. Food Res.* **2013**, *57*, 1055−1066.

DOI: 10.1021/jf505075n
J. Agric. Food Chem. XXXX, XXX, XXX−XXX

(42) Legette, L.; Ma, L.; Reed, R. L.; Miranda, C. L.; Christensen, J. M.; Rodriguez-Proteau, R.; Stevens, J. F. Pharmacokinetics of xanthohumol and metabolites in rats after oral and intravenous administration. *Mol. Nutr. Food Res.* **2012**, *56*, 466−474.

(43) Youdim, K. A.; Shukitt-Hale, B.; Joseph, J. A. Flavonoids and the brain: interactions at the blood-brain barrier and their physiological effects on the central nervous system. *Free Radical Biol. Med.* **2004**, *37*, 1683−1693.

(44) Wilson, A. J.; Kerns, J. K.; Callahan, J. F.; Moody, C. J. Keap calm, and carry on covalently. *J. Med. Chem.* **2013**, *56*, 7463−7476.

DOI: 10.1021/jf505075n
J. Agric. Food Chem. XXXX, XXX, XXX−XXX